Journal of
MATERIALS RESEARCH

Measuring the interface stress: Silver/nickel interfaces

D. Josell and J.E. Bonevich
National Institute of Standards and Technology, Gaithersburg, Maryland, 20899

I. Shao and R.C. Cammarata
The Johns Hopkins University, Baltimore, Maryland

(Received 11 May 1999; accepted 12 August 1999)

Interface stress is a surface thermodynamics quantity associated with the reversible work of elastically straining an internal solid interface. In a multilayered thin film, the combined effect of the interface stress of each interface results in an in-plane biaxial volume stress acting within the layers of the film that is inversely proportional to the bilayer thickness. We calculated the interface stress of an interface between {111} textured Ag and Ni on the basis of direct measurements of the dependence of the in-plane elastic strains on the bilayer thickness. The strains were obtained using transmission x-ray diffraction. Unlike previous studies of this type, we used freestanding films so that there was no need to correct for intrinsic stresses resulting from forces applied by the substrate that can lead to large uncertainties of the calculated interface stress value. Based on the lattice parameters of the bulk, pure elements, an interface stress of -2.02 ± 0.26 N/m was calculated using the x-ray diffraction results from films with bilayer thicknesses greater than 5 nm. This value is somewhat smaller than previous measurements obtained from as-deposited films supported by substrates. For smaller bilayer thicknesses the apparent interface stress becomes smaller in magnitude, possibly due to a loss of layering in the specimens.

I. INTRODUCTION

It is axiomatic that as layers in a solid with a laminate microstructure become thinner, interfaces become more important. For the materials scientist concerned with the thermodynamics of interfaces, one of the important quantities is the interface free energy. For simplicity, this quantity is frequently described as the cost of breaking bonds within bulk specimens of the two adjacent materials minus the energy of rejoining some, or all, of those bonds to create the interface. In fact, this described quantity is the interface excess energy (or simply interface energy); it is only when terms for the excess volume and entropy of the interface have been appropriately included that one truly is describing the interface free energy. The structure of the materials near the interface can differ from that in the bulk, specifically interatomic and interplanar spacings. In particular, interface energy, volume, and entropy can be affected. The driving force for such changes is always reduction of the free energy associated with the material as a whole, i.e. both the interface as well as all material constrained to deform with it. The free energy change of the interface arising from this change of in-plane lattice parameter is quantified by the interface stress.[1–3]

We note that it is the interface free energy that is required for understanding "high-temperature" effects where creation of new interface is possible due to atomic diffusion. Examples include grain boundary wetting, grain boundary grooving, and zero creep of multilayer thin films. However, when interface area is altered by elastic deformation, the work to deform the interface is associated with the interface stress. Thus, if only elastic deformations are possible (e.g., because the deformation occurs at a temperature below that where creep processes operate) then the relevant interface thermodynamic parameter is the interface stress. The interface stress, in addition to deposition stresses, will determine the elastic strains within the layers of the (kinetically constrained) equilibrium structure. It is the trade off of reduced interface free energy versus increased volume strain energy density within the bulk of adjacent material that matters is this case.

Conceptually the interface stress effect is straightforward to measure. Theory for measuring interface stresses in completely generalized geometry has been published by Weissmüller and Cahn.[4] Theory for multilayer films adhering to a substrate[5,6] agrees with these generalized results. For such specimens, the average bi-

axial stress σ applied to the film by the substrate must equal the biaxial volume stress within the layers $\langle\sigma\rangle$ *plus* the contribution of interface stress f for the two interfaces for each bilayer thickness λ, giving[5,6]

$$\sigma = \langle\sigma\rangle + \frac{2}{\lambda} f \quad . \tag{1}$$

The quantity f represents the interface stress f, generally a second rank tensor, which is assumed here to be isotropic. For films on a substrate it is necessary to make two measurements for each specimen: substrate curvature measurements to obtain the average stress σ applied to the film and transmission x-ray diffraction (XRD) to obtain the volume stress $\langle\sigma\rangle$ from the strains within the layers.

For a freestanding thin film, no force is applied to the film, thus $\sigma = 0$ and Eq. (1) yields

$$f = -\frac{\lambda}{2}\langle\sigma\rangle \quad , \tag{2}$$

eliminating the need for the curvature experiment and any associated errors. The interface stress f is obtained by measuring the in-plane strains in the layers of the freestanding multilayer thin films, converting these strains to forces per unit width of film using biaxial moduli of the bulk materials and then thickness averaging. Any imbalance of the forces in the layers of the freestanding film arises from the interface stress and is proportional to the interface stress and the number of interfaces. This suggests the straightforward technique of fabricating multilayer thin films with different layer thicknesses, measuring the in-plane lattice parameters, and looking for an imbalance of force that is inversely proportional to the layer thickness, i.e., proportional to the number of interfaces per unit thickness of film.[7]

Literature

Although the above method for measuring the interface stress would appear to be the simplest possible, practical considerations arising from the thickness of most multilayer specimens have precluded this approach. Instead, past measurements of the interface stress in Ag/Ni multilayers by Ruud *et al.*[6] and, subsequently, by Schweitz *et al.*[8] have been limited to specimens that were still attached to the substrates on which they had been fabricated. In both cases, correction for the force applied by the substrate to the film was accomplished using standard wafer curvature techniques to measure the curvature of the substrate, which was related to the applied force in the manner first used by Stoney[9] in 1909 (modified for biaxial stress). In their studies, the in-plane strains arising from this substrate–film interaction were as large as those arising from the interface stress; even the *sign* of the strains (and of the interface stress) varied with layer thickness prior to the correction. Although it would appear to be straightforward to quantify the errors associated with such measurements, substantial discrepancies existed. Specifically, as the layer thickness became very large, the interface effect did not go to zero.

Ruud *et al.*[6] obtained the interface stress for the Ag/Ni interfaces from the slope of their $\langle\sigma\rangle$ versus $1/\lambda$ data. Their data are anomalous in that the measured volume stress $\langle\sigma\rangle$ apparently induced by the interfaces approaches −0.5 GPa as the density of interfaces goes to zero, i.e., at large λ. Their volume stress $\langle\sigma\rangle$ is linear in $1/\lambda$ for 4.0 nm $< \lambda <$ 15 nm (0.067 nm^{-1} $< 1/\lambda <$ 0.25 nm^{-1}), allowing for the −0.5 GPa offset (Fig. 8 of Ref. 6). The volume stress decreases for $\lambda <$ 4 nm. The value of interface stress obtained from the linear region of the data is −2.27 ± 0.67 N/m. The data of Schweitz *et al.*[8], also for Ag/Ni multilayers, exhibit similar features, yielding the nearly identical value −2.24 ± 0.21 N/m. Both authors calculated the volume stress from strains relative to the lattice parameters of the pure, bulk elements.

Rodmacq[10] found that the measured strains of the Ag{220} plane spacing for multilayers up to $\lambda =$ 10.9 nm were best fit by a single value of strain within the bulk of each layer plus a much larger value of strain in the layer immediately adjacent to the interface. His fit to his Ag{220} strain data is included (later) in our Fig. 2. He did not publish his Ni{220} strain data. Some of Rodmacq's multilayer specimens were studied using the $\sin^2\psi$ technique to determine the Ag and Ni stress-free lattice parameters.[11] This technique measures atomic plane spacings at a range of orientations ψ from the specimen normal to determine the lattice parameters that would be measured if the in-plane stresses were zero. For Ag layers more than 4 monolayers thick, the stress-free lattice parameter of the Ag was found to match the lattice parameter of bulk Ag. For Ni layers 4 monolayers thick, the stress-free lattice parameter of the Ni was 1.9% larger than the lattice parameter of bulk Ni, and this difference was 0.4% for Ni layers 30 monolayers thick. The source of this behavior was not known although interface effects and/or impurities and defects were noted to be possible explanations.[11]

The $\sin^2\psi$ technique was used in conjunction with wafer curvature experiments to determine interface stresses in Au/Ni multilayers.[12,13] As with the Ag/Ni multilayers studied by the $\sin^2\psi$ technique, the measured stress-free Ni lattice parameter differed from the lattice parameter of bulk Ni. Incorporation of Au into the Ni layers due to surface segregation during growth was proposed as a possible reason for the difference. The Au atomic concentrations necessary to explain the Ni lattice parameter data were between 9 and 20%. The room-temperature, equilibrium solubility of Au in bulk Ni is <1%. An interface stress of 1.7 ± 0.1 N/m was obtained for the Au/Ni interfaces.[13]

Clemens and Eesley[14] studied Mo/Ni, Pt/Ni, and Ti/Ni multilayers on substrates using symmetric reflection XRD and wafer curvature. They observed, in all cases, an expansion of the average out-of-plane spacing that correlated with the inverse bilayer thickness, $1/\lambda$. They noted that a constant nonbulk value of the atomic plane spacing at the interface could account for this dependence. If correct, this is consistent with the concept of lattice relaxation (the out-of-plane component in this case) to lower the interface free energy. This is the basis for the interface stress.

An analysis of stresses and strains in Mo/Ni multilayers was published by Bain *et al.*[15] Although they studied specimens with $\lambda = 1$ to 20 nm, comparison of wafer curvature with XRD derived stresses was only done for the $\lambda = 10$ and 20 nm specimens. Unlike other published works, they assumed the local in-plane stresses to be *anisotropic* within each of the constituent layers. They stated that their results did not indicate a constant nonbulk value of the plane spacing at the interface as noted by Clemens and Eesley[14] for Mo/Ni interfaces. Rather, they noted that comparison of the wafer curvature and XRD results (for the $\lambda = 10$ and 20 nm specimens) implied an insignificant interface stress. However, they noted that the stresses deduced from their XRD experiments depended on their choice of principal axes. Furthermore, symmetric (measured) and asymmetric (calculated) XRD results for the out-of-plane spacing for the $\lambda = 20$ nm specimen differed significantly.

The value of interface stress published by Shull and Spaepen[16] for interfaces between {111} textured Ag and Cu layers is -0.21 ± 0.1 N/m. They utilized an *in situ* wafer curvature setup to measure the jump in substrate curvature during deposition of an interface. They used Stoney's[9] relationship between force and substrate curvature, modified for biaxial stress, to relate the jump in curvature to the interface stress. They did not measure the strains within the layers.

It is worth commenting on the use, by some authors, of the stress-free lattice parameter, as determined from the $\sin^2 \psi$ techinque, for determining interface stresses. If, for a particular specimen, the change in stress-free lattice parameter is in fact due to intermixing, then it is certainly reasonable to attempt to correct for the associated change of bulk lattice parameter by using the stress-free lattice parameter when determining the strains. However, if the behavior of the stress-free lattice parameter simply reflects out-of-plane relaxation near the interface to lower the interface free energy, then it is appropriate to use the bulk lattice parameter to determine the strains. Whether intermixing is, in fact, significant must be determined on a specimen by specimen basis. Comparison of the value of interface stress obtained in this work with the values obtained by Ruud *et al.* and Schweitz *et al.* (for validation of the new technique) requires use of the same reference states for strain calculations, i.e., the lattice parameters of the pure, bulk elements.

II. EXPERIMENT

Textured Ag/Ni(111) multilayer films with total thicknesses ranging from approximately 1.2 to 3.5 μm were fabricated for the x-ray diffraction studies on freestanding thin films. For this purpose, two liquid-nitrogen cold stages were used. These were placed along the symmetry axis of the deposition system, equidistant and equiangular from the Ag and Ni sources, at two different distances, "close" to and "far" from the sources, to permit specimens with two different bilayer thicknesses to be fabricated simultaneously. The deposition system has three shuttered electron beam sources as well as an ion source for substrate cleaning prior to deposition. Base vacuum was $<2 \times 10^{-6}$ Pa prior to deposition, and vacuum during deposition was in the mid to high 10^{-5} Pa range. Shuttering of two of the sources to obtain elemental layering on glass substrates was based on feedback from a quartz crystal oscillator and programmed controller unit. A layer of Cu or Au was deposited on the substrates from the third source prior to deposition of the multilayer (thickness <1% of the total thickness of the multilayer) permitting the films to be removed from the substrates in moist air. In previous studies of sputter-deposited Ag/Ni multilayers, glass[10] and Si[6,8] have been used as substrate materials. Our technique for removing the films from the substrates restricted us to glass substrates.

Layers in films deposited on glass microscope slides were found to be discontinous, with grains bridging layers of like material through pinholes in the intervening layer. This indicated significant mobility of the impinging atoms during growth of the films in spite of the liquid-nitrogen cold stage. Use of thin glass coverslips as substrates resulted in continuous layers. The specimens did exhibit grain boundary grooves, the groove depth increasing toward the film surface. This was most pronounced with specimens grown on the closer cold stage and was possibly a result of thermal gradients in the substrates caused by radiant energy from the molten metal sources used in electron beam evaporation. This effect was not noted to be an issue for sputter-deposited films on either Si or glass.[6,8,10]

A polycarbonate transmission holder was fabricated to hold the specimens during the transmission x-ray diffraction measurements of the in-plane lattice parameters in the Ag and Ni layers. Polycarbonate was chosen because it gave no diffraction features for scattering angles in the range of interest. The thin film specimen was placed between the two halves of the holder. Beveled transmission holes, drilled through each half of the holder, were lined up on the opposite sides of the film to permit un-

shielded access (egress) of the x-rays to (from) the circular region of thin film while still holding the specimen reasonably flat. The 3-mm hole diameter limited peak broadening from transmission geometry induced defocus, as well as film bowing, while still providing sufficient diffracting volume (i.e., signal intensity). The x-ray line source was centered parallel to the line of five transmission holes to minimize the defocus. Over the relevant range of scattering angles, broadening due to the transmission geometry induced defocus is calculated to convert a nominally zero degree width peak to a peak with an experimental full width at half-maximum (FWHM) of approximately 0.6–0.7°. Calibration of the diffractometer and transmission stage was accomplished by placing double-sided adhesive tape coated with lanthanum hexaboride powder (NIST Standard Reference Material 660) in the transmission stage. Diffraction peaks were broadened from 0.085° fwhm in reflection geometry to 0.9° FWHM in transmission geometry due to the defocus. They were, however, centered within 0.01° of the reference values within the relevant range of scattering angles. Deconvolution of the raw data from the Ag/Ni multilayers to remove this broadening was not done, as it did not affect the peak locations.

Figure 1 shows representative XRD scans (Cu K_α radiation) for Ag/Ni multilayers spanning the range of bilayer thickness studied. Specimens grown on the close stage exhibited Ag{311} and Ag{222} peaks in addition to the expected Ni{220} (bulk value 76.366° with Cu $K_{\alpha 1}$ radiation) and Ag{220} (bulk value 64.426°)[17] expected in symmetric transmission XRD scans for the [111] textured films. Specimens from the far stage typically exhibited only a weak Ag{311} peak in addition to the expected {220} peaks. This indicated higher texturing in the far stage specimens as the {220} planes studied lie at 90° from [111], hence their appearance in the symmetric transmission scans, while the {311} and {222} planes lie 80° and 70° from [111], respectively. The dependence of grooving on the cold stage used, the source of the difference in texture, has already been discussed. The grooving of the layers is not believed to have a significant effect on the measurements inasmuch as the only locations where diffraction by the {220} planes is recorded by the detector are those locations where the normals to the layers are within a few degrees of the film normal.

We summarize the Ag{220} and Ni{220} in-plane strain data obtained from the x-ray scans in Fig. 2. Because of overlapping of the Ni{220} peak with the Ag{311} peak arising from imperfect texturing, the fitting of peaks was done twice. For the first fitting the software was permitted to optimize the angles and shapes of all peaks independently (using a Pearson 7 model of each peak). For the second fitting, the scattering angles of the Ag{311} and {222} peaks were constrained to agree with the strain indicated by the Ag{220} peak of the first scan (which trended smoothly toward higher angles, smaller in-plane spacing, with decreasing bilayer thickness). Data for which the Ni{220} strain differed by more than ±0.005 (0.5°), as indicated by the two fitting procedures, were excluded (3 specimens); the majority of the data differed by less than ±0.0015 (0.15°). The Ni

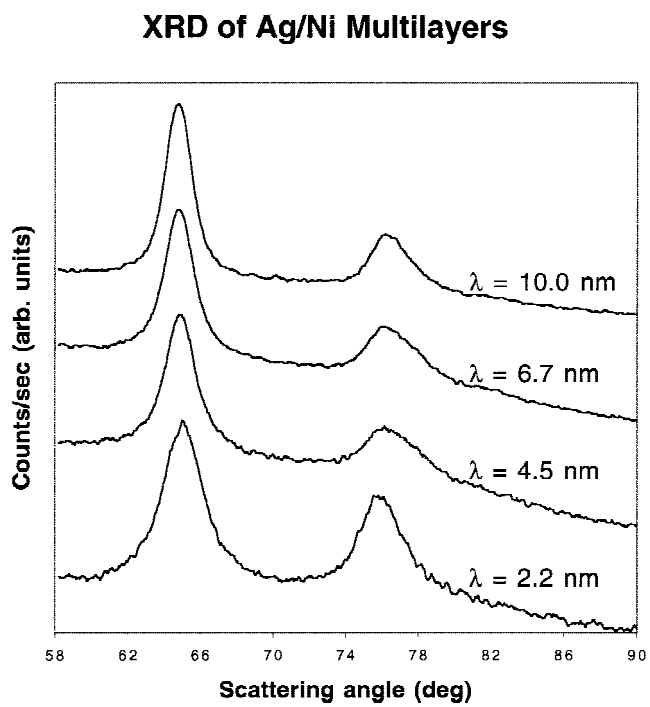

FIG. 1. X-ray diffraction scans obtained in symmetric transmission geometry on Ag/Ni multilayer thin films showing diffraction peaks rising from the Ag- and Ni{220} planes whose normals lie in the plane of the films. Note the Ag{311} peak on the high-angle shoulder of the Ni{220} peak.

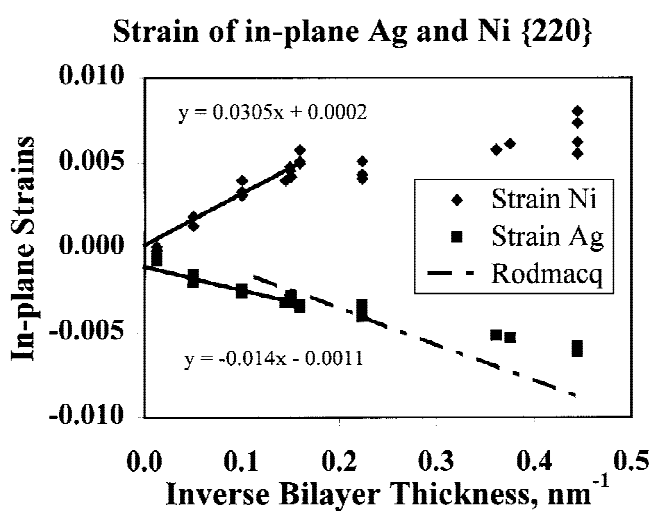

FIG. 2. Summary of the Ag and Ni in-plane strain data obtained from shifts of the {220} x-ray diffraction peaks with changing bilayer thickness.

strain data in Fig. 2 are those obtained with the constrained Ag{311} and {222} peak locations. The impact of the overlapping Ag peaks on the determination of the Ni{220} peak location manifested in the scatter of the Ni{220} strain data. The Ag{220} strain results published by Rodmacq[10] are also shown. They were also obtained from free-standing sputter-deposited Ag/Ni multilayers. He did not publish Ni{220} strain data.

III. DISCUSSION

A. Interface stress determination

The interface stress was obtained from the in-plane strain results. First, nonlinear (strain-dependent) elastic moduli were used to obtain the stresses in the Ag and Ni layers. The nonlinear biaxial elastic moduli appropriate for the texturing of the films, as given by Ruud *et al.*[6]

$$M_{Ag}(\epsilon) = 173.60 - 3764.9\epsilon - 16349\epsilon^2(\text{GPa})$$
$$M_{Ni}(\epsilon) = 389.32 - 4903.9\epsilon - 17006\epsilon^2(\text{GPa}) \quad , \tag{3}$$

were used, although the terms quadratic in strain ϵ were found to be insignificant. The stresses were multiplied by the appropriate layer thickness to obtain the force associated with each layer. The layer thicknesses were obtained from the average compositions of the films, determined using energy dispersive x-ray spectroscopy with elemental standards, and the bilayer thickness λ. The bilayer thickness was measured directly on one specimen of each bilayer period by transmission electron microscopy. Note that the target ratio of Ag layer thickness to Ni layer thickness during deposition was 1.0. The measured ratio was within 15% of this value for all films included in this study.

The interface stress f was determined from the strain and microstructure data using Eq. (2). To express Eq. (2) in terms of the experimental quantities, note that the stress in each layer is related to the strain ϵ in the layer by

$$\sigma_{Ag} = M_{Ag}\epsilon_{Ag}$$
$$\sigma_{Ni} = M_{Ni}\epsilon_{Ni} \quad , \tag{4}$$

where the nonlinear biaxial moduli M come from Eq. (3). The volume stress $\langle\sigma\rangle$ can then be written in terms of these stresses

$$\langle\sigma\rangle = \frac{\sigma_{Ag}t_{Ag} + \sigma_{Ni}t_{Ni}}{t_{Ag} + t_{Ni}} \quad , \tag{5}$$

where t is the layer thickness. The biaxial volume stress $\langle\sigma\rangle$ associated with the strain data in Fig. 2, calculated using Eq. (5), is plotted in Fig. 3(a). Using Eqs. (4) and (5), and noting that the bilayer thickness $\lambda = t_{\text{Ni}} + t_{\text{Ag}}$, Eq. (2) can be rewritten in terms of the measured strains

$$f = -\tfrac{1}{2}\left[\varepsilon_{Ag}M_{Ag}t_{Ag} + \varepsilon_{Ni}M_{Ni}t_{Ni}\right] \quad . \tag{6}$$

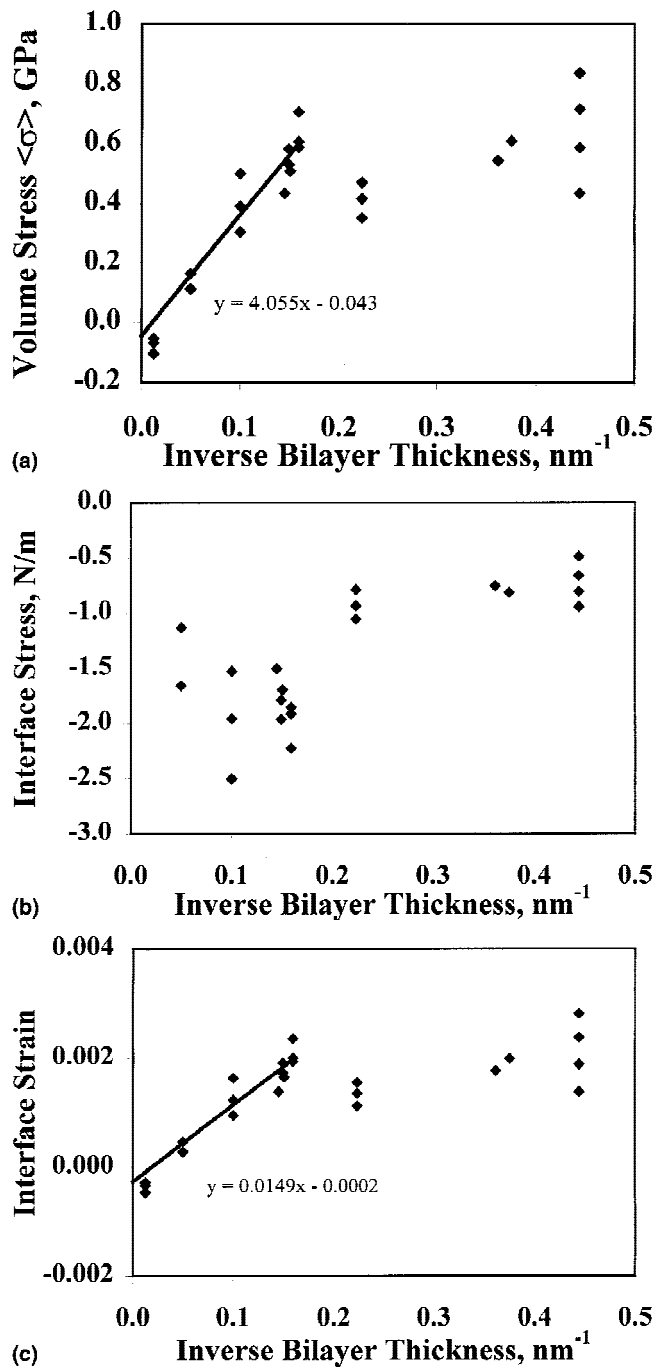

FIG. 3. (a) Biaxial volume stress determined using the Ag and Ni strain data of each specimen. (b) Interface stress determined using the Ag and Ni strain data as a function of bilayer thickness. The data for the 80-nm specimen are positive due to the nonzero offset and do not appear on the plot. (c) In-plane strain induced in each specimen by the interfaces as a function of bilayer thickness.

The interface stress f, determined from the strain data of each specimen in Fig. 2, is plotted, using Eq. (6), in Fig. 3(b). The measured interface stress varies with bilayer thickness λ. From Eq. (6), the interface stress equals the average force acting within the layers in the freestanding film. Graphically, this is *not* related to the shift of the Ag and Ni{20} diffraction peaks toward each other at small λ (Fig. 1), which simply indicates a tendency toward coherency. Rather, it is related to the shift of the point midway between the Ag and Ni peaks to lower angle (larger average in-plane lattice parameters) at small λ. In order to indicate the average strain in each specimen associated with the interface stress, the quantity

$$\epsilon_{\text{int}} = \frac{[\epsilon_{Ag} M_{Ag} t_{Ag} + \epsilon_{Ni} M_{Ni} t_{Ni}]}{[M_{Ag} t_{Ag} + M_{Ni} t_{Ni}]} \tag{7}$$

is plotted in Fig. 3(c). The specimen strain ϵ_{int} is equal to $\langle\sigma\rangle$ [Eq. (5)] divided by the average modulus of the film.

The scatter of the interface stress data [Fig. 3(b)] is largely due to the difficulties encountered in fitting the Ni{220} strain data (Fig. 2) because of the overlapping Ag{311} and {222} peaks, as discussed earlier. In contrast, the root-mean-square deviation of the Ag{220} strain data (Fig. 2) about a fit linear in λ^{-1} is less than 3×10^{-4} as its determination is not impacted by the quality of texturing. Measurements of interface stress using more highly textured freestanding films would therefore be expected to yield uncertainties significantly smaller than those presented in this work. Further improvement should also be possible by reducing the size of the transmission holes in the holder to decrease the defocus-induced peak broadening.

From Eq. (2), the slope of the $\langle\sigma\rangle$ versus $1/\lambda$ data in Fig. 3(a) yields the interface stress $f = -2.02 \pm 0.26$ N/m (stated uncertainties equal one standard deviation) in the large λ limit. In Fig. 3(b), the interface stress obtained from individual films depends on the bilayer thickness. One can obtain an average of these interface stresses for films with 5 nm $\leqslant \lambda \leqslant$ 20 nm. That value is -1.81 ± 0.34 N/m. This value does not agree with the interface stress obtained from the slope of the $\langle\sigma\rangle$ versus $1/\lambda$ data in part because of the -43 (± 69) MPa intercept of the fit to the volume stress data in Fig. 3(a). It is implicit in the individual f determinations in Fig. 3(b) that $\langle\sigma\rangle = 0$ at the large λ limit. An error has therefore been introduced in the interface stress obtained by averaging the individual values in Fig. 3(b) because of the nonzero offset value. The interface stress decreases substantially for λ less than 5 or 6 nm, going as low as -0.7 N/m for $\lambda =$ 2 nm specimens. This decrease is discussed in the next section.

B. Decrease of apparent interface stress

Due to the bowing of the substrates on which the films were deposited, low-angle reflection geometry x-ray diffraction of the multilayers was not possible. Low-angle results for the freestanding films placed on adhesive tape exhibited 1 or 2 satellites for all specimens. Micrographs

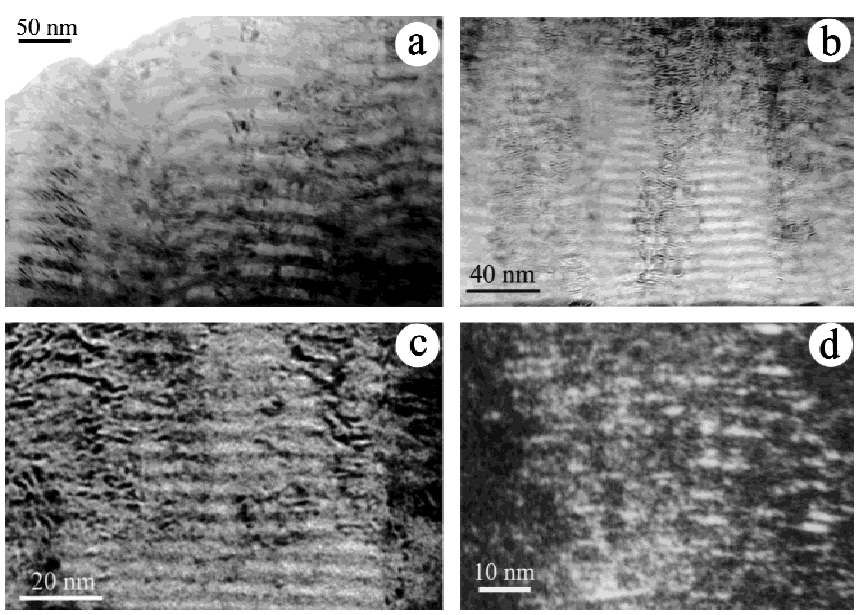

FIG. 4. Micrographs obtained by transmission electron microscopy of cross-sectioned Ag/Ni multilayers: (a) bilayer thickness 20 nm, (b) bilayer thickness 6.5 nm, (c) bilayer thickness 4.5 nm, (d) bilayer thickness 2.3 nm.

obtained by transmission electron microscopy of cross-sectioned specimens indicate that the specimens with $\lambda \geqslant 6$ nm have continuous, although not perfectly flat, layers [Figs. 4(a) and 4(b)]. Although the magnitude of the interface stress has already decreased to less than 1 N/m for the $\lambda = 4.5$ nm evaporated specimens, with the exception of grain boundary locations, the layers in these specimens also appear to be continuous [Fig. 4(c)]. Films with $\lambda = 2$ to 3 nm exhibit one low-angle x-ray diffraction satellite in reflection geometry, indicating compositional modulation, but it is unclear whether the layers are continuous [Fig. 4(d)]. Layer quality appears to affect the minimum bilayer thickness for which the single, higher value of interface stress applies: 3–4 nm for the sputtered Ag/Ni multilayers[6,8] versus 5 or 6 nm for the grooved, evaporated films of this study. A link to the interface roughness, which increases with increasing layer thickness for sputtered films,[18] could exist.

A significant change of the interface structure (dislocation density) arising from the elastic accommodation strain $\epsilon_{\mathrm{Ni}} - \epsilon_{\mathrm{Ag}}$ seems unlikely, as this strain is less than 1.4%, just one-tenth of the difference between the Ag and Ni lattice parameters, for all the specimens studied. The possibility of intermixing was raised in the studies utilizing the $\sin^2 \psi$ technique[12,13] to explain the measured stress-free lattice parameters. Such intermixing was speculatively linked to possible surface segregation during multilayer growth. Nearly identical values of the Ag/Ni interface stress were obtained using multilayers sputter-deposited on liquid-nitrogen-cooled[6] as well as water-cooled stages.[8] The value obtained in this study with Ag/Ni multilayers evaporated onto liquid-nitrogen-cooled stages is within 10% of those values. Considering the extremely different kinetics expected for the various deposition conditions, we believe that inherently kinetic effects such as intermixing and/or surface segregation are not playing a significant role in determining the value of interface stress obtained from the Ag/Ni multilayers.

C. Thermal strains

With the exception of the $\lambda = 80$ nm specimen, for which a water-cooled stage (in a different electron beam evaporation system) was used, all multilayers were deposited on substrates attached to one of the two liquid-nitrogen-cooled stages mentioned earlier. If the interfaces in the multilayer do not separate when warmed to room temperature, temperature change $\Delta T \approx 210$ K, then the difference between the elastic strains ϵ^T induced in the layers is given by

$$\epsilon^T_{Ag} - \epsilon^T_{Ni} = -\int_{77K}^{290K} (\alpha_{Ag} - \alpha_{Ni})\, \mathrm{d}T \quad , \qquad (8)$$

where α is the thermal expansion coefficient. An *approximate* value can be obtained by substituting the room-temperature values[19] $\alpha_{\mathrm{Ni}} = 13.3 \times 10^{-6}\ \mathrm{K}^{-1}$ and $\alpha_{\mathrm{Ag}} = 19.1 \times 10^{-6}\ \mathrm{K}^{-1}$ into Eq. (8). The mismatch of the elastic strain arising from the warming is thus predicted to be approximately $\epsilon^T_{\mathrm{Ni}} - \epsilon^T_{\mathrm{Ag}} = 1.2 \times 10^{-3}$. Experimentally, the strain in the Ag layers, for layer thickness extrapolated to $1/\lambda = 0$, is approximately -1.1×10^{-3} (Fig. 2). The Ni strain data extrapolate to approximately 0.2×10^{-3} (Fig. 2). Therefore, the experimental value of the mismatch strain is approximately 1.3×10^{-3}.

D. Extrapolation to stresses in infinitely thick layers

If the bulk moduli are appropriate for the thin film materials, then the biaxial volume stress $\langle\sigma\rangle$ extrapolated to $1/\lambda = 0$ should equal zero, corresponding to equal and opposite forces in the Ag and Ni layers. The actual (offset) stress from Fig. 3(c), -43 ± 69 MPa, is statistically indistinguishable from 0 MPa and less than one-tenth the offset noted earlier in the data of Ruud *et al.* Using the thickness-averaged bulk moduli, the magnitude of the uniform shift of the Ag and Ni strain data associated with the stress offset is less than 4×10^{-4}. Note that the strains in the layers of the $\lambda = 80$ nm specimen are smaller in magnitude than the linear fits (Fig. 2), consistent with the absence of the large thermal component. A stress offset of 70 MPa is also evident in these data.

IV. CONCLUSION

We have conducted transmission x-ray diffraction experiments with freestanding Ag/Ni multilayer thin films in order to measure the interface stress. Our results indicate that the interface stress for bilayer thickness greater than 5 nm is $f = -2.02 \pm 0.26$ N/m. The impact of grain boundary grooving and intermixing on this value has not been quantified. (Use of stress-free lattice parameters lowers the interface stress value obtained by Schweitz *et al.* to approximately one-third the value originally published.[8])[20] Good agreement of these results with previously published results for specimens on substrates demonstrates the equivalence of these techniques when identical reference states (e.g., lattice parameters of pure, bulk elements) are used. Because the films were detached from their substrates, wafer curvature measurements were not necessary, making these measurements considerably simpler than those of other studies as well as removing a source of error. Furthermore, the small scatter of the Ag strain measurements indicates that this technique has the potential to provide interface stress values with uncertainties significantly smaller than those obtained here. This improvement should be readily achievable by studying more highly textured specimens and decreasing the size of the holes in the transmission stage to decrease the peak broadening caused by defocus.

ACKNOWLEDGMENTS

We thank Frans Spaepen, Kasper Schweitz, Olivier Thomas, and Bruce Clemens for helpful comments. Work done by D. Josell was supported, in part, by DOE/OBES Award No. DEFG0297ER45664. Work at Johns Hopkins University was supported by the Materials Research Science and Engineering Center as administered by the National Science Foundation.

REFERENCES

1. J.W. Cahn, Acta Metall. **28,** 1333 (1980).
2. J.W. Cahn and F. Larche, Acta Metall. **30,** 51 (1982).
3. R.C. Cammarata, Prog. Surf. Sci. **46,** 1 (1994).
4. J. Weissmüller and J.W. Cahn, Acta Mater. **45A,** 1899 (1997).
5. D. Josell, Acta Metall. Mater. **42,** 1031 (1994).
6. J.A. Ruud, A. Witvrouw, and F. Spaepen, J. Appl. Phys. **74,** 2517 (1993).
7. This experiment was proposed independently to D. Josell by J. Weissmüller and R.C. Cammarata.
8. K.O. Schweitz, H. Geisler, J. Chevallier, J. Bøttiger, and R. Feidenhans'l, in *Thin Films-Stresses and Mechanical Properties VII,* edited by R.C. Cammarata, M.A. Nastasi, E.P. Busso, and W.C. Oliver (Mater. Res. Soc. Symp. Proc. **505,** Warrendale, PA, 1998), p. 559.
9. G.G. Stoney, Proc. R. Soc. **82,** 72 (1909).
10. B. Rodmacq, J. Appl. Phys. **70,** 4194 (1991).
11. K-F. Badawi, N. Durand, Ph. Goudeau, and V. Pelosin, Appl. Phys. Lett. **65,** 3075 (1994).
12. G. Gladyszewski, S. Labat, P. Gergaud, and O. Thomas, Thin Solid Films **319,** 78 (1998).
13. S. Labat, O. Thomas, P. Gergaud, A. Charai, C. Alfonso, L. Barrallier, B. Gilles, and A. Marty, J. Phys. IV **6,** C7–135 (1996).
14. B.M. Clemens and G.L. Eesley, Phys. Rev. Lett. **61,** 2356 (1988).
15. J.A. Bain, L.J. Chyung, S. Brennan, and B.M. Clemens, Phys. Rev. B **44,** 1184 (1991).
16. A.L. Shull and F. Spaepen, J. Appl. Phys. **80,** 6243 (1996).
17. Card Nos. 04-0850 (Ni) and 64-0783 (Ag), JCPDS-International Center for Diffraction Data V. 1.30 (1997).
18. K.O. Schweitz (unpublished).
19. *Smithells Metals Reference Book,* edited by E.A. Brandes (Butterworths, London, 1983), p. 14-1.
20. K.O. Schweitz (unpublished).